

## Research Article

## Accelerated Homogenization of a Cast Nickel-Based Superalloy VDM780 via Thermomechanical Processing

H. Chavilian, S.H. Razavi, B. Mohammad Sadeghi\*, H.R. Abedi and S.M. Abbasi

School of Metallurgy &amp; Materials Engineering, Iran University of Science and Technology (IUST), Tehran, Iran

## ARTICLE INFO

*Article history:*

Received 10 June 2025

Reviewed 14 July 2025

Revised 25 July 2025

Accepted 18 August 2025

*Keywords:*

Nickel-base superalloy VDM780

Hot rolling

Homogenization

Microstructure

*Please cite this article as:*

Chavilian, H., Razavi, S. H., Mohammad Sadeghi, B., Abedi, H. R., & Abbasi, S. M. (2025). Accelerated homogenization of a cast nickel-based superalloy VDM780 via thermomechanical processing. *Iranian Journal of Materials Forming*, 12(3), 33-41.

<https://doi.org/10.22099/IJMF.2025.53481.1334>

## ABSTRACT

In recent years, the push to reduce fuel consumption and emissions in turbines, designs have focused on achieving higher operating temperatures, which require materials capable of sustaining elevated temperatures in industrial applications. The development and production of the nickel-base superalloy VDM780, with an operating temperature above 750 °C (nominally 780 °C), have been pursued to meet this demand. This superalloy is often considered a suitable alternative to Inconel 718. The present study demonstrates the thermomechanical processing can significantly accelerate homogenization, enabling the production of a wrought structure in VDM780 with minimal heat treatment. A cast ingot of the VDM780 superalloy was first prepared using a vacuum induction melting (VIM) furnace, without employing refining processes such as electroslag remelting (ESR) or vacuum arc remelting (VAR). The conditions for homogenization and hot rolling were then investigated using simultaneous thermal analysis (STA). The results show that a homogenization temperature of 1160 °C provides adequate homogenization, resulting in a microstructure that is well-suited for workability.

© Shiraz University, Shiraz, Iran, 2025

### 1. Introduction

VDM780 is a wrought nickel-based superalloy introduced in 2014, designed to retain the good workability of IN718 alloy while extending its usability to high temperatures (above 650 °C). Although initially introduced as a "new type IN718", the similarity between the two alloys is limited to their comparable workability.

The high strength of VDM780 originates from  $\gamma'$ -Ni<sub>3</sub>(Al, Ti) precipitates, whereas IN718 achieves its strength primarily through  $\gamma''$  precipitates. This difference in the strengthening phase is the fundamental distinction between the two alloys and determines their operating temperature ranges. At temperatures of VDM780 (above 650 °C), the  $\gamma''$  strengthening phase in IN718 becomes

\* Corresponding author

E-mail address: [bmsadeghi@iust.ac.ir](mailto:bmsadeghi@iust.ac.ir) (B. Mohammad Sadeghi)<https://doi.org/10.22099/IJMF.2025.53481.1334>

unstable, resulting in a significant reduction in strength. Consequently, alloy VDM780 exhibits greater similarity to Waspaloy, as both share comparable operating temperatures and rely on  $\gamma'$  precipitates for strengthening. However, the development of VDM780 addresses a major shortcoming of Waspaloy. The primary drawback of Waspaloy is the narrow thermal window, approximately 15 °C, between the dissolution temperatures of  $\gamma'$  and  $M_{23}C_6$  phases, which severely restricts its workability [1, 2].

In this new superalloy (later named VDM780), efforts were made to develop a suitable replacement for IN718 for industrial applications such as aerospace and land-based gas turbines, with a minimum operating temperature of 750 °C and a formability window exceeding 100 °C [3].

In addition to the  $\gamma'$  phase, which primarily contributes to the high-temperature strength of the superalloy, another phase aids in grain refinement. In early studies on VDM780, this phase was identified as  $\delta$ - $Ni_3Nb$  with a D0a crystal structure. However, more recent investigations using high-resolution transmission electron microscopy have also identified the ordered  $\eta$ - $Ni_6AlNb$  phase, which forms a layered structure with discrete  $\eta$  and  $\delta$  particles [4, 5]. The formation of this phase is significantly slower compared to the  $\gamma'$  phase, indicating that longer heat treatment processes are required for its precipitation. Notably, no studies to date have reported the presence of carbides in VDM780. Therefore, to strengthen grain boundaries and prevent grain growth, it is critical to generate sufficient high-temperature precipitates during heat treatment [6].

Following the completion of research by Federova and other members of the research team comprising experts from VDM and the Technical University of Braunschweig, industrial property rights and a U.S. patent for the nickel-based superalloy, commercially known as VDM780, were registered in 2015. Shortly thereafter, European and Japanese patents were also secured for this superalloy. Due to the interest garnered from certain industrial manufacturers, a German patent for the composition of the VDM780 superalloy was registered in 2020 [7, 8].

In a study on VDM780 conducted by Solis and colleagues [9], the presence of the  $\gamma$  matrix and the strengthening  $\gamma'$  phase was confirmed, with no evidence of the  $\gamma''$  phase under any heat treatment conditions. Generally, the dissolution of  $\gamma'$  begins at 800 °C, and by 970 °C, no trace of the  $\gamma'$  phase remains. As a result of this dissolution, Al and Nb, the primary constituents of  $\gamma'$ , become integrated into the  $\gamma$  matrix. Since their atomic sizes are larger than those of Ni, Cr, and Co (the main elements forming the  $\gamma$  matrix), they significantly strengthen the matrix phase and increase the lattice parameter of  $\gamma$  [10, 11].

In a study focusing on the physical properties of welded VDM780 samples, scanning electron microscopy (SEM-EDS) revealed precipitates of Nb-rich particles and eutectic  $\gamma$ /Laves phases [12]. However, investigations of solution-annealed wrought samples showed no precipitates indicating the potential to eliminate these precipitates through appropriate heat treatment [13].

Other research findings indicate that in the VDM780 superalloy,  $\delta$  and  $\eta$  precipitates form both as plates and as fine layers alongside each other to stabilize grain boundaries. This behavior was further clarified through transmission electron microscopy (TEM) studies, which identified three distinct phases in addition to the  $\gamma$  matrix. The  $\gamma'$  phase appears as cubic precipitates, while the  $\delta$  and  $\eta$  phases can form individually or coexist within the matrix. The  $\delta$  and  $\eta$  phases exhibit blocky morphologies but may also form as layered structures within the same region, making them difficult to distinguish in such configurations [14].

Regarding the nature and composition of plate-shaped precipitates, studies using high-resolution TEM images have examined the structure of blade-like precipitates in the VDM780 superalloy. These studies revealed that the blades consist simultaneously of  $\delta$  and  $\eta$  phases. It was reported that these two phases form in a layered arrangement with distinct structures, orthorhombic for  $\delta$  and hexagonal for  $\eta$ , within the plate-shaped phase boundary. These blades display a simultaneous distribution of both precipitates, making differentiation between them challenging [4, 5].

Other investigations into the formability of the VDM780 superalloy reported a significant presence of twins in the initial wrought structure and an average grain size of approximately 20  $\mu\text{m}$  for industrially produced samples [3, 15, 16]. Studies comparing the effect of microstructure on the mechanical properties of VDM780 with other common superalloys highlighted its relative superiority. These studies noted that if forming and heat treatment conditions are optimized to control the  $\gamma$  matrix grain size and  $\gamma'$  precipitate distribution, the alloy's strength, due to achieving a fine-grained structure, can surpass that of many industrial superalloys [17, 18].

Investigating into the hot deformation behavior of VDM780 in the temperature range of 1000 to 1150  $^{\circ}\text{C}$  emphasized the significant influence of dynamic and post-dynamic recrystallization. In some cases, maintaining the deformed sample at high temperatures for only a few minutes after deformation resulted in a several-fold increase in the recrystallized fraction [19, 20].

Most studies on this superalloy have utilized wrought samples as the starting material. Limited research has addressed the as-cast microstructure of the VDM 780 superalloy, and there remains a significant research gap concerning the homogenization process and the transformation of the as-cast structure into a wrought microstructure. This study makes a novel contribution by employing as-cast ingots instead of forged ones, focusing on homogenization through thermomechanical processing, and offering a new perspective on enhancing the alloy's microstructural properties.

The primary objective of this study was to identify suitable conditions for transforming a vacuum induction melted (VIM) cast sample into a wrought component without the use of electroslag remelting (ESR) or vacuum arc remelting (VAR). To achieve this, a thermomechanical cycle was designed to perform sequential homogenization and hot rolling, thereby

fabricating a wrought material from the VDM780 superalloy.

## 2. Experimental Procedure

For laboratory casting and production of the VDM780 superalloy, a vacuum induction furnace ( $10^{-3}$  mbar) was used. The chemical composition of the alloy was verified using a spark optical emission spectrometer. The chemical composition of the ingot obtained after VIM casting is presented in Table 1. As shown, the measured composition is in close agreement with the reported values for this superalloy [7–9].

To determine suitable temperatures for heat treatment and homogenization, a STA SDT650 device was used with a heating rate of 10  $^{\circ}\text{C}/\text{min}$  up to 1300  $^{\circ}\text{C}$ .

Fig. 1 illustrates the thermomechanical process employed for forming the VDM780 superalloy. The thermomechanical processing was carried out using an electric resistance furnace for both homogenizing (preheating) and reheating between deformation passes. The sample temperature was carefully monitored and controlled throughout the forming process using a laser pyrometer to ensure precision. After each deformation pass, the sample was rapidly transferred (within 10 seconds) back to the furnace to facilitate post-dynamic recrystallization. The forming process was performed on a two-high rolling mill over five consistent passes, with a constant strain rate of 4  $\text{s}^{-1}$  maintained across all passes. After the final pass, the sample was air-cooled to ambient temperature. A temperature of 1160  $^{\circ}\text{C}$  was selected for two primary reasons: first, based on the STA analysis results, it was found to be suitable for homogenization and elimination of the as-cast structure; second, it serves as an appropriate preheating temperature between rolling passes. During rolling, the sample typically experiences a temperature drop of approximately 50 to 60  $^{\circ}\text{C}$  upon exiting the furnace and being placed under the rolling mills. Therefore, by utilizing a preheating temperature of 1160  $^{\circ}\text{C}$ , the sample temperature during forming was

**Table 1.** Mean chemical composition of the VDM780 superalloy cast ingot produced in a VIM furnace (wt. %)

Element	Ni	Co	Nb	Mo	Cr	Al	Ti	Zr
Studied material	48.3	24.07	5.12	2.77	17.3	2.31	0.47	0.007
Ref. [9]	Bal.	25	5.4	3	18	2	0.2	-

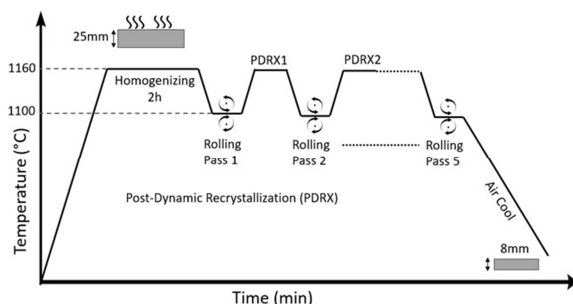


**Fig. 1.** Schematic illustration of the thermomechanical processing applied to the VDM780 superalloy. The time axis is designed as a notional representation without a specific temporal scale.

maintained in the range of 1080–1120 °C. According to previous studies, this range is optimal for the deformation of this superalloy, enabling both dynamic and post-dynamic recrystallization [19, 20].

Scanning electron microscopy (Philips) and X-ray diffraction (Tongda TD3700) were employed for further analysis. X-ray diffraction (XRD) analysis was performed to characterize the crystallographic structure of the samples, using a copper (Cu) target with a characteristic  $K\alpha$  radiation wavelength of 1.5406 Å (Cu  $K\alpha 1$ ). The XRD measurements were conducted with a step size of 0.04°, an operating voltage of 40 kV, and a current of 30 mA. Data were collected over a  $2\theta$  range of 40° to 110° to capture the primary diffraction peaks relevant to phase identification and structural analysis. The diffraction patterns were subsequently analyzed to determine phase composition, lattice parameters, and crystallographic orientation, ensuring a comprehensive evaluation of the material's microstructural properties. For metallographic analysis, the sample underwent grinding and polishing processes using diamond paste, followed by etching with a solution of HCl (60 vol.%) and HNO<sub>3</sub> (40 vol.%).

### 3. Results and Discussion

To better understand the as-cast structure, both the microstructure and macrostructure of the ingot were examined. As shown in Fig. 2(a), a columnar structure is present along the ingot's edges, while equiaxed grains are observed at the center. Figs. 2(b) and (c) display microstructural images of the cast ingot at two magnifications, revealing dendritic blade structures and

interdendritic phases. These observations are consistent with previous reports on VIM-cast ingots of superalloys [21].

For improved identification of precipitates and interdendritic phases, SEM-EDS images were utilized. The resulting image and chemical composition of the matrix and interdendritic phases are presented in Fig. 3. According to this figure (Fig. 3(c)), the matrix contains 45.1 wt.% Ni and 9.2 wt.% Nb, which aligns relatively well with the weight percentages reported in Table 1. This suggests that the matrix phase exhibits only minor compositional variations, while interdendritic phases are enriched in Nb (Figs. 3(b) and (d)). Similar precipitates reported in previous studies are likely associated with  $\gamma$ /Laves eutectic phases [12].

To determine the suitable temperature and duration for homogenization and hot rolling, STA analysis was performed. As shown in Fig. 4, points 1 and 2 correspond to the dissolution of the  $\gamma'$  phase at approximately 915 °C and the dissolution of eutectic phases and undissolved particles at around 1170 °C, respectively. The  $\gamma'$  dissolution temperature obtained here is consistent with values reported in previous studies [3, 13, 14].

Despite differences in casting methods, thermomechanical cycles, and forming conditions compared to prior studies, the similarity in material behavior properties at these temperatures validates the

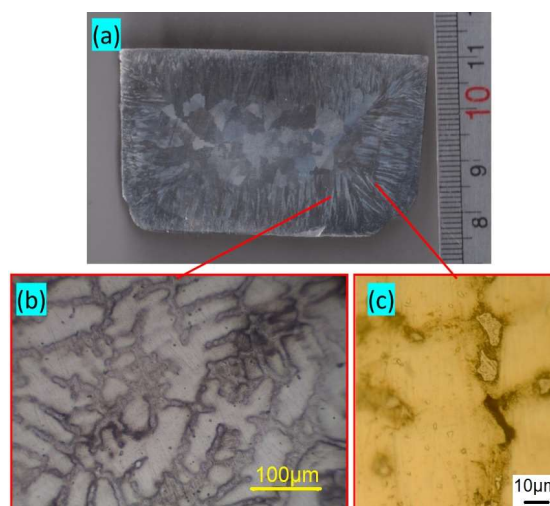


**Fig. 2.** As-cast structure of the VDM780 superalloy ingot: (a) macrostructure, and (b, c) microstructures at different magnifications.

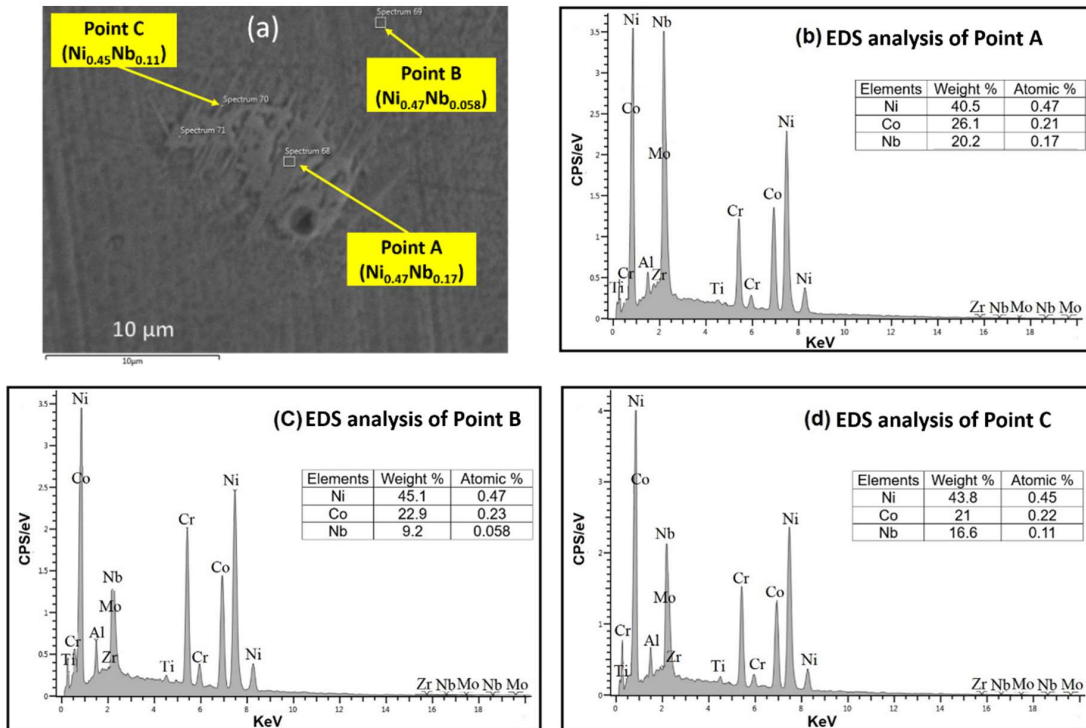


Fig. 3. (a) SEM image and (b-d) EDS analysis for three points of the VDM780 superalloy cast ingot produced in a VIM furnace.

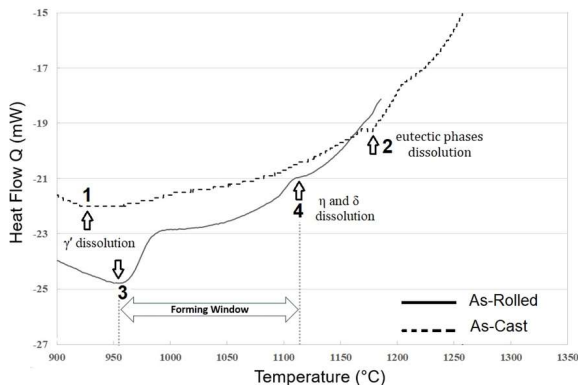


Fig. 4. STA analysis of cast and hot-rolled VDM780 superalloy samples in the temperature range 900 to 1300 °C at a heating rate of 10 °C/min.

effectiveness of the optimized processing route developed in this study. By integrating deformation and heat treatment within a streamlined thermomechanical cycle, and eliminating additional refining steps (such as ESR & VAR), wrought components with microstructural and mechanical characteristics comparable to conventionally forged parts were successfully produced. This demonstrates the potential of the proposed abbreviated process to deliver high-quality materials while enhancing production efficiency.

Based on the STA analysis results, a homogenization treatment at 1160 °C for 2 hours was selected, followed immediately by hot rolling. A total deformation of 70% was achieved in five stages, with 5-minute intervals between each stage to allow for post-dynamic recrystallization (PDRX). After forming, the sample was air-cooled (Fig. 1). Fig. 5 shows an optical microscopy image of the hot-rolled sample, revealing an average grain size of approximately 20 μm and a hardness of about 520 HV30.

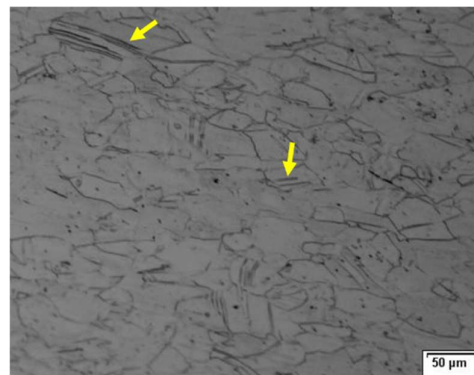


Fig. 5. Microstructural image of the VDM780 superalloy after hot rolling at 1160 °C with a 70% reduction. Arrows indicate the presence of twins.

The hardness of the as-cast specimen was measured at 348 HV30 prior to deformation. Following thermomechanical processing, which involved hot rolling and subsequent heat treatment, the hardness increased markedly to 520 HV30. This improvement can be attributed to several microstructural changes induced by processing. During hot rolling, plastic deformation leads to the formation of a refined grain structure and increased dislocation density. Additionally, thermomechanical treatment promotes dynamic and post-dynamic recrystallization, producing fine grains and stabilizing the newly formed grain boundaries [17]. The combined effects of grain refinement, higher dislocation density, and the elimination of casting defects are likely responsible for the observed increase in hardness from 348 HV30 to 520 HV30.

In Fig. 5, the presence of twins and the obtained grain size are consistent with wrought samples produced by forging in previous studies [3, 15, 18]. Although a full mechanical property evaluation was beyond the scope of this study, the hardness obtained (520 HV30) is comparable to values reported for wrought VDM780, suggesting acceptable transformation from cast to wrought structure.

As observed in Fig. 5, no traces of dendritic structures or interdendritic phases are observed. The elimination of undissolved particles and eutectic phases is further supported by the STA analysis results in Fig.

4. Points 3 and 4 in Fig. 4 correspond to the dissolution of  $\gamma'$  (around 950 °C) and high-temperature  $\eta$  and  $\delta$  precipitates (around 1100 °C), respectively. The temperature range between points 3 and 4 is recognized as the forming window for the VDM780 superalloy, consistent with values reported in previous studies [6, 7]. Additionally, the absence of heat flow changes above 1100 °C confirms the lack of undissolved particles and eutectic phases.

The X-ray diffraction (XRD) results for the hot-rolled sample are presented in Fig. 6. As observed, the known precipitates in the VDM780 superalloy, previously identified in other diffraction studies, are also present in the hot-rolled sample [9, 10]. The absence of peaks corresponding to interdendritic compounds and eutectic phases indicates the successful formation of a suitable wrought structure and the complete elimination of the original VIM cast structure. The material obtained in this study can serve as an appropriate wrought blank for further investigations into solution annealing and aging treatments of the VDM780 superalloy. The elimination of the as-cast structure and the development of a wrought microstructure after hot rolling can be attributed to the concurrent application of homogenization and hot deformation process. Previous studies have shown that hot deformation can promote the removal of the dendritic structure in cast components [22].

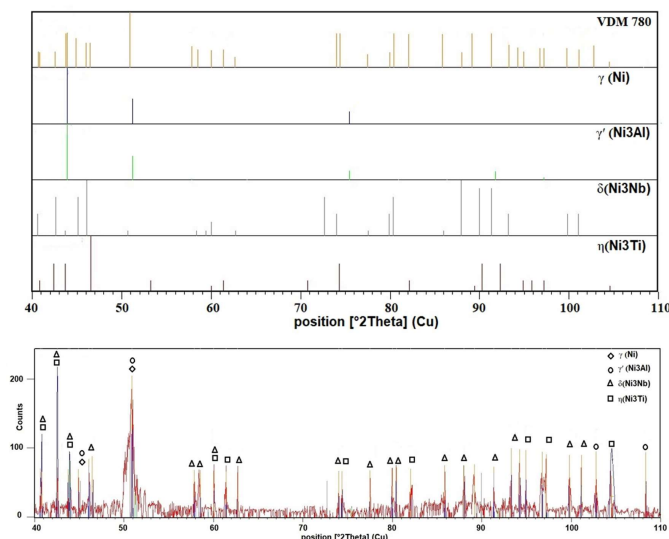


Fig. 6. X-ray diffraction (XRD) patterns of the VDM780 superalloy sample after hot rolling.



In the present alloy, the elimination of the cast structure is mainly attributed to the combined effects of homogenization and hot deformation. Hot deformation accelerates homogenization by introducing a high dislocation density and facilitating dynamic and post-dynamic recrystallization. During hot rolling, severe plastic deformation produces a large number of dislocations, which serve as fast diffusion paths for alloying elements [23]. These dislocation networks increase atomic mobility and significantly enhance diffusion kinetics compared to static heat treatment, where diffusion relies only on thermal activation. Additionally, dynamic recrystallization during hot deformation promotes the formation of fine, equiaxed grains, which further refining the microstructure and disrupt the dendritic network. Post-dynamic recrystallization, occurring during cooling, stabilizes the new grain boundaries and reduces chemical inhomogeneities. Together, these mechanisms enhanced diffusion through dislocations and recrystallization-driven refinement results in a faster and more effective elimination of the cast structure compared to static annealing, where such dynamic processes do not occur [24].

Furthermore, due to the multi-stage nature of the hot rolling process within the thermomechanical cycle employed in this study, the initial workpiece, after deformation and before the next pass, was held at high temperature for a short period of time to facilitate the conditions for post-dynamic recrystallization. Haghighat et al. [19, 20] reported that in the VDM780 superalloy, the recrystallized fraction in the deformed material exhibits a significant increase after only a few minutes of exposure to high temperatures.

#### 4. Conclusions

In this study, a wrought sample of the VDM780 superalloy was successfully produced from a laboratory-scale VIM-cast ingot. The as-cast dendritic structure and interdendritic precipitates were characterized through microstructural analysis and electron microscopy analysis. Simultaneous thermal analysis (STA) up to 1300 °C was employed to determine suitable

temperature for homogenization and preheating temperature of 1160 °C for two hours was selected, followed by hot rolling with a total 70% reduction. The resulting hot-rolled, microstructure exhibited an average grain size of approximately 20 µm and a hardness of 520 HV30. XRD and STA analyses confirmed the complete elimination of the dendritic structure and eutectic phases. This study demonstrates that, despite differences in casting and thermomechanical processing routes, the developed streamlined cycle, integrating deformation and heat treatment while avoiding refining steps (such as ESR & VAR), produces wrought components with properties comparable to conventionally forged parts, underscoring an efficient approach to obtaining high-quality materials.

#### Authors' contributions

**Hooman Chavilian:** Conceptualization, Investigation, Validation, Writing - Review & Editing

**Seyed Hosein Razavi:** Conceptualization, Methodology, Supervision

**Bagher Mohammad Sadeghi:** Conceptualization, Methodology, Review & Editing, Supervision

**Hamid Reza Abedi:** Conceptualization, Methodology, Supervision

**Seyed Mahdi Abbasi:** Conceptualization, Funding acquisition, Project administration, Methodology, supervision

#### Conflict of interest

The authors declare that they have no known competing financial interests or personal relationships that could have appeared to influence the work reported in this paper.

#### Funding

The authors thank the Iran University of Science and Technology (IUST) for the financial support of this study.

#### 5. References

- [1] Fedorova, T., Rösler, J., Klöwer, J., & Gehrmann, B. (2014). Development of a new 718-type Ni-Co superalloy family for high temperature applications at 750 °C. In *MATEC Web of Conferences* (Vol. 14, p.

- 01003). EDP Sciences.  
<https://doi.org/10.1051/mateconf/20141401003>
- [2] Fedorova, T., Rösler, J., Gehrmann, B., & Klöwer, J. (2014, November). Invention of a new 718-type Ni-Co superalloy family for high temperature applications at 750 °C. In *8th International Symposium on Superalloy 718 and Derivatives* (pp. 587-599). Hoboken, NJ, USA: John Wiley & Sons, Inc.  
<https://doi.org/10.1002/9781119016854.ch46>
- [3] Rösler, J., Hentrich, T., & Gehrmann, B. (2019). On the development concept for a new 718-type superalloy with improved temperature capability. *Metals*, 9(10), 1–20.  
<https://doi.org/10.3390/met9101130>
- [4] Sharma, J., Nicolaÿ, A., De Graef, M., & Bozzolo, N. (2021). Phase discrimination between  $\delta$  and  $\eta$  phases in the new nickel-based superalloy VDM Alloy 780 using EBSD. *Materials Characterization*, 176, 111105.  
<https://doi.org/10.1016/j.matchar.2021.111105>
- [5] Ghica, C., Solís, C., Munke, J., Stark, A., Gehrmann, B., Bergner, M., Rösler, J., & Gilles, R. (2020). HRTEM analysis of the high-temperature phases of the newly developed high-temperature Ni-base superalloy VDM 780 premium. *Journal of Alloys and Compounds*, 814, 152157. <https://doi.org/10.1016/j.jallcom.2019.152157>
- [6] Bergner, M., Rösler, J., Gehrmann, B., & Klöwer, J. (2018, May). Effect of heat treatment on microstructure and mechanical properties of VDM Alloy 780 premium. In *Proceedings of the 9th International Symposium on Superalloy 718 & Derivatives: Energy, Aerospace, and Industrial Applications* (pp. 489-499). Cham: Springer International Publishing. [https://doi.org/10.1007/978-3-319-89480-5\\_31](https://doi.org/10.1007/978-3-319-89480-5_31)
- [7] Gehrmann, B., Kloewer, J., Fedorova, T., & Roesler, J. (2015). *Nickel-cobalt alloy* (U.S. Patent Application No. US20150354031A1). United States Patent and Trademark Office.  
<https://patents.google.com/patent/US20150354031A1>
- [8] Gehrmann, B., Hentrich, T., Schmidt, C., & Brunnert, K. (2021). *Nickel-cobalt alloy powder and method of manufacturing the powder* (German Patent Application No. DE102020116868A1). German Patent and Trademark Office.  
<https://patents.google.com/patent/DE102020116868A1/en>
- [9] Solís, C., Munke, J., Bergner, M., Kriele, A., Mühlbauer, M. J., Cheptiakov, D. V., Gehrmann, B., Rösler, J., & Gilles, R. (2018). In situ characterization at elevated temperatures of a new Ni-based superalloy VDM-780 premium. *Metallurgical and Materials Transactions A*, 49(9), 4373–4381. <https://doi.org/10.1007/s11661-018-4761-6>
- [10] Kümmel, F., Fritton, M., Solís, C., Kriele, A., Stark, A., & Gilles, R. (2022). Near-surface and bulk dissolution behavior of  $\gamma'$  precipitates in nickel-based VDM® alloy 780 studied with in-situ lab-source and synchrotron X-ray diffraction. *Metals*, 12(7), 1067.  
<https://doi.org/10.3390/met12071067>
- [11] Fritton, M., Nagel, O., Kümmel, F., Stark, A., Hafez Haghighat, M., Gehrmann, B., Neumeier, S., & Gilles, R. (2025). Post hot-deformation precipitation behavior of  $\gamma'$  phase in VDM® alloy 780 under varying cooling rates and aging temperatures: An in situ high energy XRD study. *Journal of Alloys and Compounds*, 1037, 182111.  
<https://doi.org/10.1016/j.jallcom.2025.182111>
- [12] Ariasetta, A., Sadeghinia, N., Andersson, J., & Ojo, O. (2023). Keyhole TIG welding of newly developed nickel-based superalloy VDM Alloy 780. *Welding in the World*, 67(1), 209–222. <https://doi.org/10.1007/s40194-022-01425-y>
- [13] Solís, C., Kirchmayer, A., da Silva, I., Kümmel, F., Mühlbauer, S., Beran, P., Gehrmann, B., Hafez Haghighat, M., Neumeier, S., & Gilles, R. (2022). Monitoring the precipitation of the hardening phase in the new VDM® alloy 780 by in-situ high-temperature small-angle neutron scattering, neutron diffraction and complementary microscopy techniques. *Journal of Alloys and Compounds*, 928, 167203.  
<https://doi.org/10.1016/j.jallcom.2022.167203>
- [14] Kirchmayer, A., Weiser, M., Randelzhofer, P., Freund, L. P., Gehrmann, B., Hafez Haghighat, M., Huenert, D., Göken, M., & Neumeier, S. (2023). Oxidation behavior of the polycrystalline Ni-base superalloy VDM® alloy 780. *Metallurgical and Materials Transactions A*, 54(5), 1961–1970. <https://doi.org/10.1007/s11661-022-06956-z>
- [15] Kümmel, F., Kirchmayer, A., Solís, C., Hofmann, M., Neumeier, S., & Gilles, R. (2021). Deformation mechanisms in Ni-based superalloys at room and elevated temperatures studied by in situ neutron diffraction and electron microscopy. *Metals*, 11(5).  
<https://doi.org/10.3390/met11050719>
- [16] Hou, K., Ou, M., Xing, W., Ma, G., Hao, X., Wang, M., & Ma, Y. (2024). The formation of  $\eta$ -Ni<sub>3</sub>Ti phase microstructure in a cast nickel-based superalloy with high Ti/Al ratio. *Journal of Materials Research and Technology*, 29, 764–778.  
<https://doi.org/10.1016/j.jmrt.2024.01.156>
- [17] Hardy, M. C., Hafez Haghighat, M., Argyrakakis, C., Buckingham, R. C., La Monaca, A., & Gehrmann, B. (2023, March). The effect of microstructure on the strength of VDM alloy 780. In *TMS Annual Meeting & Exhibition* (pp. 29-47). Cham: Springer Nature Switzerland.
- [18] Vaasudevan, A., León-Cázares, F. D., Fischer, E., Witulski, T., Rae, C., & Galindo-Nava, E. (2023). Towards enhancing hot tooling to form high- $\gamma'$



- superalloys. *Minerals, Metals and Materials Series*, 718, 65–91. [https://doi.org/10.1007/978-3-031-27447-3\\_5](https://doi.org/10.1007/978-3-031-27447-3_5)
- [19] Sharma, J., Hafez Haghighat, M., Gehrmann, B., Moussa, C., & Bozzolo, N. (2020, August). Dynamic and post-dynamic recrystallization during supersolvus forging of the new nickel-based superalloy—VDM alloy 780. In *Superalloys 2020: Proceedings of the 14th International Symposium on Superalloys* (pp. 450–460). Cham: Springer International Publishing. [https://doi.org/10.1007/978-3-030-51834-9\\_44](https://doi.org/10.1007/978-3-030-51834-9_44)
- [20] Hafez Haghighat, M., Sharma, J., Gehrmann, B., Alves, H., & Bozzolo, N. (2023). Supersolvus recrystallization and grain growth kinetics for the fine tuning of grain size in VDM alloy 780 forgings. *Metallurgical and Materials Transactions A*, 54(5), 2092–2111. <https://doi.org/10.1007/s11661-023-07018-8>
- [21] Forbes Jones, R. M., & Jackman, L. A. (1999). The structural evolution of superalloy ingots during hot working. *JOM*, 51(1), 27–31. <https://doi.org/10.1007/s11837-999-0007-9>
- [22] Raza, S. S., Ahmad, T., Kamran, M., Zhang, X., Basit, M. A., Manzoor, M. U., Inam, A., Butt, O. M., & Abrar, M. (2020). Effect of hot rolling on microstructures and mechanical properties of Ni base superalloy. *Vacuum*, 174, 109204. <https://doi.org/10.1016/j.vacuum.2020.109204>
- [23] Błoniarczyk, R., Majta, J., Rutkowski, B., Korpala, G., Prah, U., Janiszewski, J., & Lisiecka-Graca, P. (2021). How the thermomechanical processing can modify the high strain rate mechanical response of a microalloyed steel. *Materials*, 14(20), 1–17. <https://doi.org/10.3390/ma14206062>
- [24] Wan, Z. P., Shen, J. Y., Wang, T., Wei, K., Li, Z., Yan, S., Liu, M., & Hu, L. X. (2022). Effect of hot deformation parameters on the dissolution of  $\gamma'$  precipitates for as-cast Ni-based superalloys. *Journal of Materials Engineering and Performance*, 31(2), 1594–1606. <https://doi.org/10.1007/s11665-021-06276-0>